ISSN 1063-780X, Plasma Physics Reports, 2024, Vol. 50, No. 3, pp. 331–341. © Pleiades Publishing, Ltd., 2024.

OSCILLATIONS AND WAVES IN PLASMA

# The Frequency Spectrum and Energy Content in a Pulse Flux of Terahertz Radiation Generated by a Relativistic Electron Beam in a Plasma Column with Different Density Distributions

**A. V. Arzhannikov[a,*], S. L. Sinitsky[a], D. A. Samtsov[a,**], I. V. Timofeev[a], E. S. Sandalov[a], S. S. Popov[a], M. G. Atlukhanov[a], M. A. Makarov[a], P. V. Kalinin[a], K. N. Kuklin[a], A. F. Rovenskikh[a], and V. D. Stepanov[a]**

[a] *Budker Institute of Nuclear Physics, Siberian Branch, Russian Academy of Sciences (BINP SB RAS), Novosibirsk, 630090 Russia*

**e-mail: A.V.Arzhannikov@inp.nsk.su*

***e-mail: D.A.Samtsov@inp.nsk.su*

Received November 21, 2023; revised December 27, 2023; accepted December 28, 2023

**Abstract**—This paper reports on the generation of a directed flux of electromagnetic radiation with an energy content of 10 J in the frequency range of 0.2–0.3 THz at a microsecond pulse duration in a beam–plasma system. The flux is generated when a relativistic electron beam (REB) pumps electron plasma waves in a magnetized plasma column. In the described experiments, this fundamentally new approach to generate terahertz radiation was carried out at the GOL-PET facility in the conditions of varying the beam current density and the plasma density in the appropriate ranges of 1–2 kA/cm$^2$ and $10^{14}$–$10^{15}$ cm$^{-3}$. From the comparison of the flux energy spectrum measured experimentally in the frequency range 0.15–0.45 THz with the calculated one obtained using the previously proposed model of radiation generation in a beam–plasma system it was shown that this process occurs through resonant pumping by REB of precisely the branch of upper-hybrid plasma waves. Mastering this new method to generate terahertz radiation opens the prospect of its use to obtain multi-megawatt radiation fluxes in the frequency range up to 1 terahertz and higher. For such a development approach the most promising beam for pumping plasma oscillations seems to be a kiloampere REB generated in a linear induction accelerator.

**Keywords:** relativistic electron beam, plasma column, beam–plasma interaction, waves in plasma, terahertz radiation, megawatt radiation flux

**DOI:** 10.1134/S1063780X24600051

## INTRODUCTION

Terahertz radiation has the ability to spread through substances and various materials that are opaque in the optical and infrared ranges, simultaneously exciting vibrational modes of supramolecular structures and crystal lattices of solids, as well as rotational levels of complex molecular formations. The presence of these properties leads to more active use of terahertz radiation in various areas of human activity, such as diagnosis of various conditions of human tissues and organs without a harmful effect on living subjects [1]. The terahertz range is also important for creating radar systems with the ability to visualize small hidden objects [2] and spectroscopy and excitation of phonon vibrations in molecular crystals and supramolecular structures [3]. Thus, the development and creation of high-power sources of electromagnetic radiation in the terahertz frequency range (0.1–10 THz) is one of the priority tasks of modern physics.

In our opinion, one of the promising approaches to generate high-power radiation fluxes in the frequency range of 0.1–0.9 THz is to use the mechanisms of intense beam–plasma interaction [4] and the further transformation of plasma oscillations pumped by the beam into electromagnetic waves from the plasma, as it was assumed to explain bursts of radiation coming from the solar corona [5]. In the case where electron beams with a particle energy of ~1 MeV and a current in the range of 1–10 kA [4], the power of which reaches the gigawatt level are used, one can expect the generation of terahertz radiation fluxes with a power on a scale of tens and even hundreds of MW. Mastering this new method to generate radiation makes it possible to significantly expand the range of applications of high-power radiation fluxes of the frequency

range 0.1–1 THz. It is important to emphasize that the use of this beam–plasma mechanism in the terahertz spectral region opens a unique opportunity to quickly change the frequency of the generated radiation flux by varying density of the plasma. Experimental studies in this direction started at the GOL-3 facility in the Budker Institute of Nuclear Physics Siberian Branch, Russian Academy of Sciences, using an electron beam with an energy up to 1 MeV, a beam current of 10–15 kA, and a pulse duration of 5 μs, which was injected into a magnetized plasma column [6]. In experiments on the relaxation of a high-current relativistic electron beam (REB) in a plasma column with a density of $\sim 10^{14}$ cm$^{-3}$, the features of the radiation flux for the spectral range 0.1–0.5 THz escaping in the direction normal to the magnetic field lines were established [7, 8]. Based on the results of these and further studies, the mechanisms of the radiation generation were identified. One of these mechanisms is the excitation of upper-hybrid plasma oscillations by the electron beam followed by their subsequent transformation on plasma density gradients into the flux of electromagnetic radiation at the frequency of this branch of plasma waves [8–11]. Another mechanism occurs during a nonlinear process of two upper-hybrid oscillations merge into one electromagnetic wave with a frequency equal to double the value of the oscillation frequency of the origin [5, 12, 13]. During the experiments, it was found that the transverse emission of electromagnetic radiation at the indicated frequencies is localized at distances on a scale of 1 meter from the point of the beam injection into the plasma column, which corresponds to the relaxation length of the REB in the plasma [14]. Subsequent experiments carried out at the GOL-PET facility demonstrated that the increase of the plasma density results in redirecting the radiation flux from the normal to the plasma column to the one along its axis [15]. In further studies at the GOL-PET facility, the regularities of influence of plasma density gradients on the spectral composition and the power of the generated radiation flux were established. In the same experiments a new mechanism for the flux generation during the beam interaction with the plasma was discovered, which occurs in the following way. In the presence of a regular periodic structure of density gradients in plasma, direct pumping by the beam the branch of electromagnetic oscillations in the plasma is possible [10, 11]. In the experiments, conditions to provide effective output of the radiation flux from the plasma column end into a vacuum, which propagates along the axis of the beam–plasma system were determined. As well, during the experiments the necessary conditions for effective output of the radiation flux from the vacuum chamber into the atmosphere of the experimental hall through a dielectric polymer window [16, 17] were found. Moreover, the results of these experiments allowed us to carry out our first measurements of the energy content in the radiation flux with a microsecond pulse duration [18]. These measurements have shown that the high power density in the radiation flux leads to a strong pulse shortening down to 1 μs at the output into the atmosphere, while the duration of the radiation flux, measured directly in vacuum, reached 3.5 μs. We explain this phenomenon of the radiation pulse shortening in entering the atmosphere by the developing of the surface RF breakdown on the vacuum side of the output window [19].

This article is devoted to solution of the problem of preventing RF breakdown and achieving the maximum energy content in the radiation flux into the atmosphere. In order to provide detailed comparison of the generated radiation spectrum with the result of the theoretical consideration, experiments with the purposeful maintenance of a plasma density uniform over a cross-section that were practically constant during the period of generation of the radiation flux were carried out. In the article the spectral composition of the radiation flux measured under these experimental conditions and distribution of the spectral radiation power density in the frequency range of upper-hybrid plasma oscillations calculated in numerical simulation are compared.

## EXPERIMENTAL FACILITY

The described series of experiments on the generation of terahertz radiation in a beam–plasma system was carried out in the Budker Institute of Nuclear Physics Siberian Branch, Russian Academy of Sciences at the GOL-PET facility. The scheme of this facility and used diagnostics were described in detail in [16–20]; therefore, we will only briefly touch on some key aspects of this issue. The diagram of the described experiments is presented in Fig. 1.

To create an electron beam for injection into the plasma, the U-2 accelerator with a magnetically insulated diode is used. In this device the electron beam of a ribbon cross-section is generated under conditions of cathode–anode gap insulation by a magnetic field with an induction that varied in the range of 0.12–0.3 T depending on the purposes of the experiment [21]. The ribbon beam formed in the accelerating diode with a cross-section of 350 × 56 mm propagates further along a slit vacuum channel with a gap between planes of 80 mm [21]. Then it passes through the spatial region of the vacuum chamber, where its cross-section is transformed into a circular one in accordance with the geometry of guiding magnetic field lines. Finally, the beam is compressed to a diameter of 40 mm as the field induction increases to 4.3 T. Measurements have shown that using such a scheme of the beam cross-section transformation and compression, the U-2 accelerator provides injection into the plasma column of the electron beam with an energy in the range of 0.4–0.8 MeV and an angular divergence of particle velocity of 0.1 rad [22] at a pulse duration of 5 μs. In the described experiments the current density

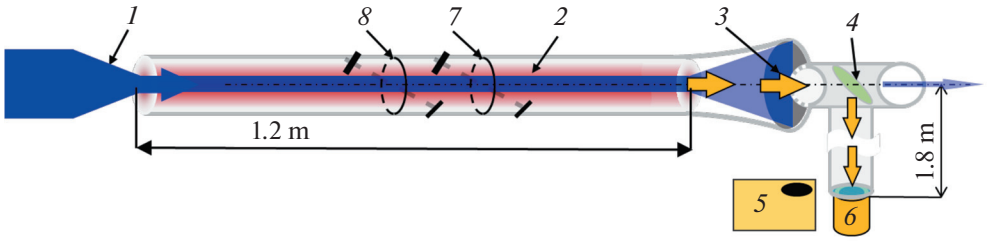


**Fig. 1.** A scheme of the plasma part of the GOL-PET facility demonstrating propagation path of the terahertz radiation flux and the location of diagnostics for its registration. (*1*) Injected REB, (*2*) plasma column, (*3*) radiation flux, (*4*) deflecting mirror, (*5*) polychromator, (*6*) calorimeter, (*7*) interferometer, (*8*) Thomson scattering.

of the beam passing through the plasma was determed by the ratio between the values of magnetic field induction in the accelerating diode and in the plasma column. It had two values: 1 and 2 kA/cm$^2$. The beam was injected into a plasma column with a diameter of 80 mm and a length of 1.2 m, confined in a solenoid with a corrugated magnetic field with the ratio of the maximum and minimum induction values $B_{max}/B_{min} = 4.5/3.2$ T. A description of the process to create a plasma column with different density distributions over the column cross-section was presented in [20]. This paper demonstrated that it is possible to create a plasma column with different density distributions, both along the column cross-section and along its length [20]. This distribution is achieved by the special choice of the conditions for pulsed injection of gas into the vacuum chamber (the moments of opening the valves and the duration of their open state), choosing the geometry of the discharge electrodes and the moment of applying a high (20 kV) voltage pulse to the discharge gap filled with gas. In addition, if the degree of ionization of the gas cloud in the vacuum chamber resulting from the high-voltage discharge current flow is far from unity, then the plasma density may increase and its distribution along the plasma column may change during the beam injection.

It should be noted that in the presence of significant radial gradients of plasma density, the pulsed power of the radiation flux generated in the beam–plasma system increases by more than an order of magnitude compared to the case of a uniform distribution of that density [11]. The article describes experiments and presents results of both density distributions over the plasma column cross-section: ingomogeneous and gomogeneos.

To measure the beam current in the diode and in the magnetic compression system, as well as the currents flowing through the individual sections of the plasma column, a set of Rogowski coils located in different sections of the vacuum chamber along the facility axis was used. It should be noted that in the case of a high (exceeding $2 \times 10^{14}$ cm$^{-3}$) plasma density along the entire length of the plasma column, the Rogowski coils surrounding the plasma column do not register any magnetic field of the beam current, since under these conditions the beam current is fully neutralized by the plasma return current.

The energy of the electrons in the beam injected into the plasma column is determined by the voltage applied to the accelerating diode. To measure the plasma density, we use infrared laser diagnostics: a Michelson interferometer at a wavelength of 10.5 μm [23], and a Thomson scattering system at a wavelength of 1.053 μm [24, 25]. Changes in plasma temperature in different sections of the plasma column during the beam injection are estimated using the signals from diamagnetic loops, which are proportional to the transverse plasma pressure.

The experiments described in this paper were focused on achievement of the maximum per pulse energy content in the radiation flux propagating along the axis of the facility and then into the atmosphere. In order to achieve this result, the radiation flux and high-current REB from the end of the plasma column are separated according to the following scheme. At the end of the plasma column, where a sharp decrease in plasma density occurs, a strong decrease in the induction of the guiding magnetic field along the axis of the facility begins. This leads to a significant cross-section expansion of the electron beam. The beam with decreased current density is absorbed by the annular graphite collector. In its turn, the radiation flux without change of its previous cross-section propagates in a metal tube to a radiation reflector made of a thin stainless steel foil. The mirror plane foil of the reflector is inclined to the facility axis at an angle of 45 degrees. After reflection, the radiation flux is directed through another metal tube whose axis is directed at an angle of 90 degrees with respect to the symmetry axis of the plasma column. Next, the radiation flux enters the atmosphere through an exit window made of polymethylpentene, which transmits terahertz radiation with low losses [26].

To record the spectral characteristics of the generated terahertz radiation flux, detectors based on Schottky barrier diodes (SBD) supplied with frequency-selective bandpass filters are used. These eight detectors together make an eight-channel polychro-

mator designed to analyze the spectral composition of the radiation flux in the frequency range from 0.1 to 0.6 THz [27]. To measure the energy content in the flux of electromagnetic radiation, a specialized calorimeter provided to us by the authors of [28] was used. The process of measuring the energy content of the radiation flux using the calorimeter is based on the electromagnetic radiation energy absorption in a thin-walled cylindrical metal-ceramic shell and recording changes in its temperature by a large number (about 1000) of thermocouples connected in series. The calorimeter responsetivity measured at a frequency of about 100 GHz, has a value of 90 μV/J, which is slightly different from the 70 μV/J measured at a frequency of 10 GHz and indicated in [28]. A description of the measurement procedure and the results of the first experimental series on measuring energy content in a pulsed flux of terahertz radiation are given in [18]. Based on the above comment on the calorimeter responsetivity measurements, we can assume that measurements of the absolute value of the energy content in the radiation flux in a single radiation pulse are provided with good reliability in our experiments. Taking into account the time dynamics and amplitude of the radiation signals recorded by the channels of the eight-channel polychromator during the pulse of generated radiation flux, we calculate the absolute value of the average power over the pulse duration in that part of the spectrum where the high spectral radiation density is localized. To indicate the distribution of the radiation flux density over the its cross-section visually, which is important for recording the percentage of the captured flux fraction in the calorimeter, panels of gas-discharge neon bulbs are used. In the cavity of the bulb a high-frequency discharge occurs when the specific flux power exceeds a threshold value, which is estimated at the level $(1–2) \times 10^4$ W/cm$^2$. The high-frequency discharge that occurs in the bulbs is uniformly distributed over the area of the polymer panel is accompanied by a bright glow. The optical image of these glowing bulbs recorded by a SSD camera brand SDU-205 indicates that the measured flux power exceeded the determined threshold level (Fig. 1 in [18]).

## THE FREQUENCY SPECTRUM AND ENERGY CONTENT IN A RADIATION PULSE AT INHOMOGENEOUS PLASMA DENSITY IN THE BEAM CROSS-SECTION

As noted above, the results of previous experiments on measuring the energy content in a pulsed radiation flux were described in [18]. During those experiments, the calorimeter was placed in the atmosphere of the experimental hall and the radiation flux exited the vacuum chamber through a teflon window with a diameter of 14 cm. The window was located at a distance of 30 cm from the metal mirror, providing flux deflection at 90 degrees in the direction transverse to the axis of the plasma column. The calorimeter was located at a distance of 60 cm from the teflon window. In this distance the cross-section of the radiation flux propagating freely in the atmosphere already reached a diameter of 30 cm. In order to direct the radiation flux to the entrance aperture of the calorimeter with a diameter of 11.5 cm, a steel tube with a diameter of 18 cm was installed between the output window and the calorimeter. The tube provided transport of the radiation flux emerging from the output window to the calorimeter entrance. In this experimental configuration breakdown along the vacuum surface of the output window limited the pulse duration of the radiation flux into the atmosphere to a level below 1 μs. The energy content in the flux captured by the calorimeter at a shortened pulse duration reached 2–2.5 J. Since the inlet aperture of the calorimeter (11.5 cm) was noticeably smaller than the diameter of the tube (18 cm), we can say that the energy content in the pulsed flux is at least no less than the indicated results of the calorimetric measurements.

To prevent RF breakdown development at the vacuum side of the output window we reconstructed the unit that transmits the radiation flux from the vacuum to the atmosphere [29]. The output window was shifted from the radiation reflector to a distance of 150 cm with a stainless steel tube 12 cm in diameter. Simultaneously, the material of the window was replaced by polymethylpentene, which is more suitable for these experiments. Unlike teflon, this new material has higher transmittance in the terahertz spectral region and it transmits light in the optical range. Increasing the distance from the reflector to the output window made it possible to reduce the hydrogen concentration near its end, which increases during the propagation of the gas flow from the area of the plasma column. Moreover, when the radiation flux is reflected by the steel mirror local areas of increased power density in the immediate vicinity, contributing to the occurrence of breakdown, occurred. When the radiation flux from the reflector propagates along a long tube, these localizations of increased power density are blurred and the probability of the high-frequency breakdown is significantly reduced.

In a recent experiment in measuring the energy content in the radiation flux into the atmosphere, the inlet aperture of the calorimeter was connected to an output window made of polymethylpentene, with a minimum gap between them. At the same time, the radiation flux transmitted through the window into the atmosphere is limited by the inner diameter of the vacuum tube of 12 cm, which only slightly exceeds the calorimeter inlet aperture of 11.5 cm diameter. During the experiments, the plasma density in the electron beam cross-section passing through the plasma column was maintained at level $4 \times 10^{14}$ cm$^{-3}$ with the radial density profile presented in Fig. 2a. The presented plasma density profile is obtained by measuring the radial plasma density distribution by Thomson scattering and averaging of the measurements over

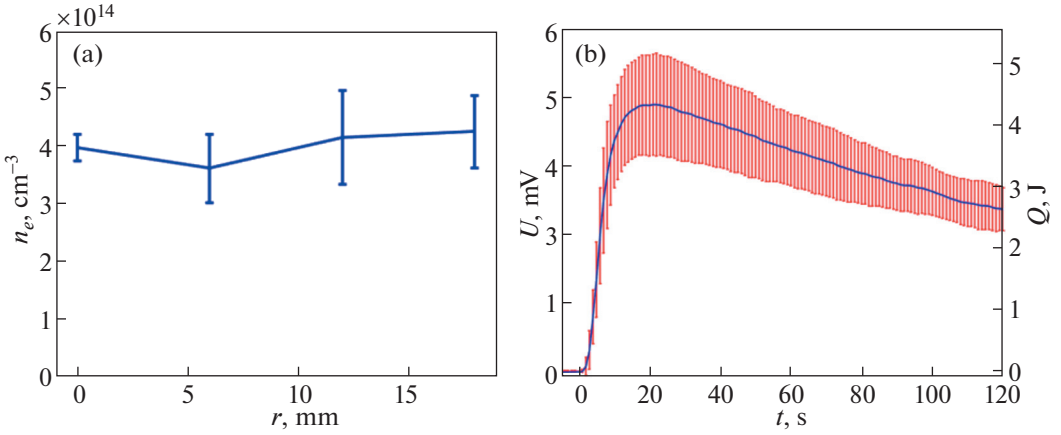


**Fig. 2.** The density distribution along the radius of the plasma column at a time of 2 μs (a) and the energy in the radiation pulse recorded by the calorimeter after the output window made of polymethylpentene (b). The results are averaged over 5 shots under identical beam and plasma conditions.

a series of five shots with the beam injection. As one can see, the time of heat propagation from the calorimeter surface absorbing radiation to the layer where the thermocouples are located has a scale value of 10 s, while the characteristic time of cooling exceeds 100 s. In accordance with the result of the absolute responsivity calibration, it can be stated that the energy content in the pulsed flux from the output window under these conditions is about 4 J.

To measure the spectral composition of radiation flux, the calorimeter was replaced by an eight-channel polychromator. Before entering the input aperture of the polychromator the radiation flux propagating from the output window was collimated to a diameter of 4 cm by a hole in the radiation-absorbing screen. Furthermore its intensity was weakened homogeneously over the entire radiation spectrum. The results of measuring the spectral composition of the radiation flux under these conditions with the polychromator are presented in Fig. 3.

First, two main local frequency bands, that is, the low-frequency band corresponding to the range of 0.14–0.16 THz, and the high-frequency band, to the range of 0.3–0.4 THz, are to be noted. The first one corresponds to the frequency region of the branch of upper-hybrid plasma oscillations extending from 0.14 to 0.19 THz, at the obtained values of the plasma density (3–4) × $10^{14}$ cm$^{-3}$ and the magnetic field induction $B = 4$ T. These electromagnetic waves are generated during the transformation of upper-hybrid plasma oscillations on plasma density gradients (see [9, 10, 13]). In turn, the high-frequency band (0.3–0.4 THz), corresponding to frequency values two times larger compared to that contained in the low-frequency band, we associate with a nonlinear process in which two upper-hybrid plasma oscillations merge into one electromagnetic wave [12, 13]. Two other frequency bands of generated radiation, at 0.11–0.12 THz and at 0.22–0.24 THz, as we believe, are associated with the harmonics of the radiation emitted by plasma electrons moving in cyclotron orbits. The fundamental frequency is $fc = eB/2\pi mc = 0.11$ THz (at $B = 4$ T) and its doubled value is 0.22 THz.

In these experiments, measurements of the energy content in the pulsed radiation flux by the calorimeter had a value of 3.5–4 J, which significantly exceeds the level of 2–2.5 J recorded in the previous series of experiments. The increase in the energy of the radiation flux captured by the calorimeter is caused by an increase in the duration of the flux pulse from the vacuum chamber into the atmosphere. As the waveforms from frequency-selective channels of the polychromator demonstrate, the pulse duration of the radiation flux reached 4 μs in this series of experiments. At the same time, it should be taken into account that the power level reaches its maximum during the first microsecond and then gradually decreases.

In order to increase the precision of the energy content measurements in the radiation pulse generated by the electron beam in the plasma column, a series of experiments was carried out with a calorimeter directly connected to the vacuum chamber instead of the output window. This was performed by removing the output window separating the working cavity of the calorimeter, where the radiation flux is absorbed, from the steel tube through which the flux propagates in vacuum. Under these conditions, pumping out the volume of the calorimeter to a high vacuum was done simultaneously with the creation of vacuum conditions in the plasma part of the facility. We note that the calorimeter body was connected to the tube through a special dielectric gasket so that there was no electrical contact between the calorimeter and the vacuum chamber of the facility. It should be recalled that the diameter of the tube through which the radiation flux propagates is 12 cm and the inlet aperture of the calo-

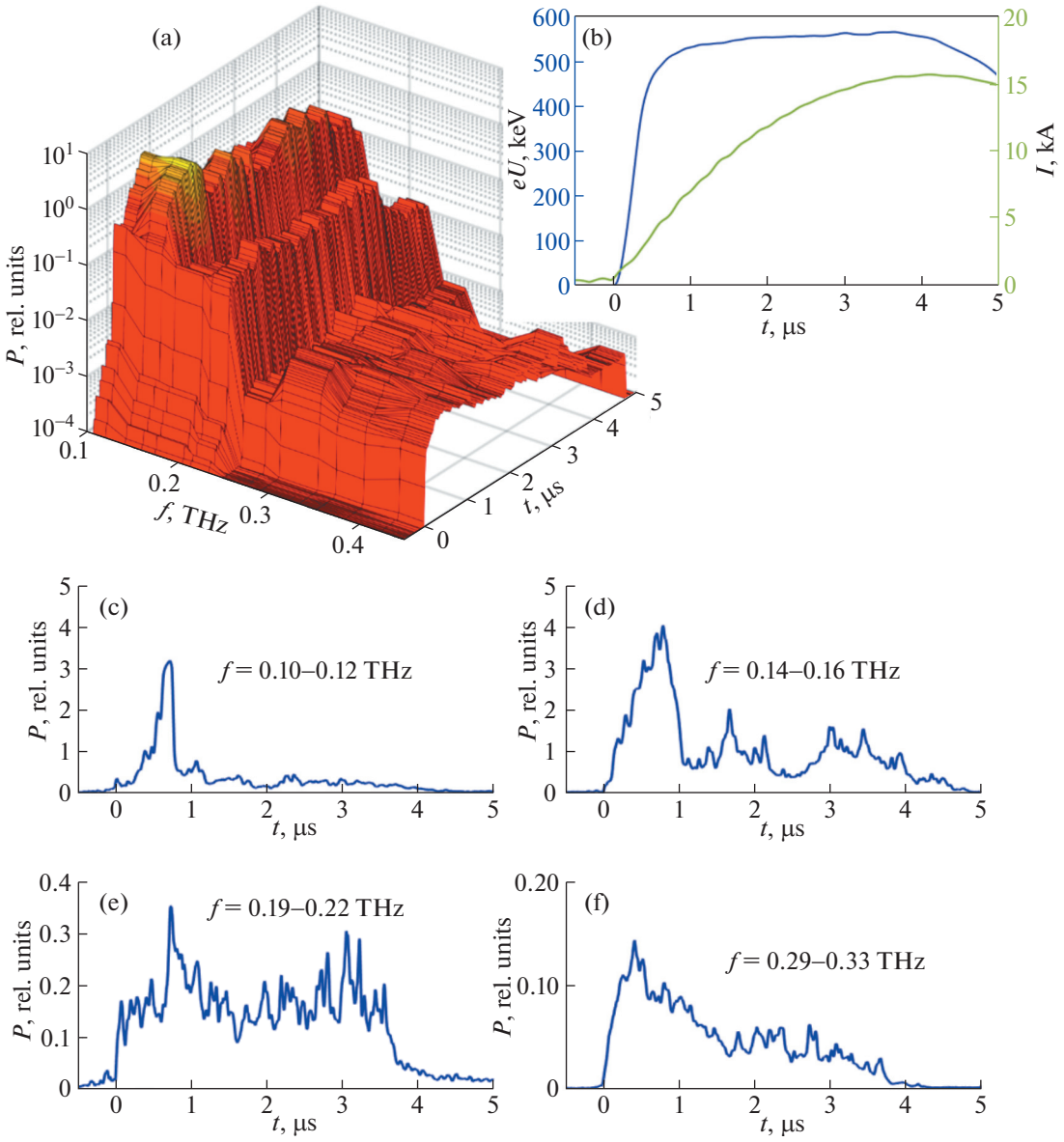


**Fig. 3.** The spectral power density in the radiation flux into the atmosphere (a) recorded by an eight-channel polychromator at a plasma density distribution shown in Fig. 2a. The ordinate axis shows the spectral radiation density in relative units presented taking into account calibration of the each channel absolute responsivity in its recording spectral region. Current of the injected electron beam and energy of electrons (b). Radiation intensity signals received from the polychromator channels in the frequency range 0.1–0.12 (c), 0.14–0.16 (d), 0.19–0.22 (e), 0.29–0.33 THz (f). All presented signals are averaged over a series of 9 shots.

rimeter is 11.5 cm. Under these conditions the small annular edge of the cross-section of the flux propagating through the tube was not captured by the calorimeter, which could lead to a slight underestimation of the energy content in the flux measured per pulse by the calorimeter.

The results on the measuring the energy of the radiation flux obtained in the described variant of the calorimeter placement are presented by the blue line in Fig. 4. It should be noted that in these experiments the diameter of the electron beam in the plasma was 4 cm. According to this beam diameter, the calculated average over the beam cross-section current density was $j_b = 1$ kA/cm$^2$. This current density was maintained in all experiments described above in the text.

The results on measuring the energy of the radiation flux obtained in the described variant of the calorimeter placement are presented by the blue line in Fig. 4. The waveforms of the voltage obtained at the thermocouples connected to the calorimeter body (Fig. 4) indicates that the temperature rise time slightly differs compared to the case with the presence of atmosphere inside the calorimeter cavity. On the

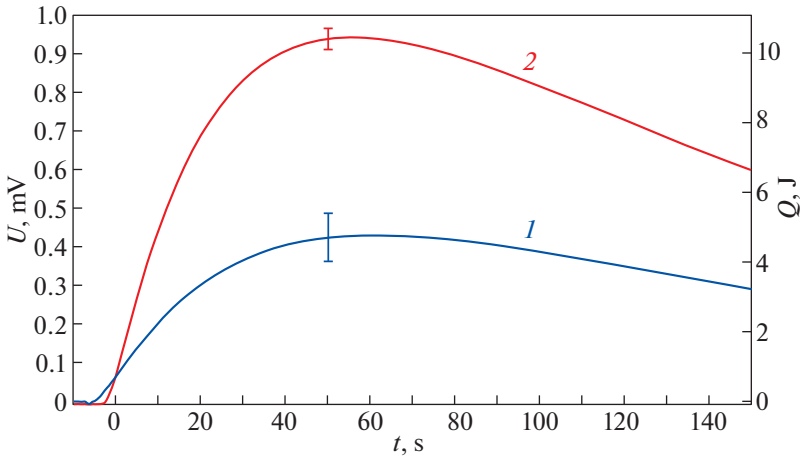


**Fig. 4.** The energy in a radiation pulse measured by a calorimeter directly connected to a vacuum tube, in the cases of the beam current density is close to 1 (curve *1*) and 2 kA/cm$^2$ (curve *2*).

other hand, in vacuum conditions in the calorimeter cavity the decrease in the temperature of the working fluid requires a much longer time than for that with atmosphere. One can state that the heat removal from the calorimeter working fluid is largely influenced by the presence of an air mass inside its cavity.

It should be noted that previously carried out experiments on plasma heating by relativistic electron beams with a pulse duration of ~100 ns showed [30] that in order to achieve a high level of pumping of the plasma oscillations at a plasma density of (4–5) × $10^{14}$ cm$^{-3}$, the beam current density in the plasma has to significantly exceed 1 kA/cm$^2$. Taking these results of previously carried out experiments into account, the current density of the beam in the plasma column in the following experiments was increased. For this the magnetic field induction in the U-2 accelerator diode was reduced from 0.25 to 0.19 T and the field induction in the plasma column was increased from 4 to 4.5 T. Such actions allowed us to increase the current density of the beam passing through the plasma column to a level of 2 kA/cm$^2$. Under these conditions, the intensity of the beam–plasma interaction did increase. The energy content in the radiation flux at its microsecond pulse duration increased by approximately two-fold for the same plasma density of 4 × $10^{14}$ cm$^{-3}$, as evidenced by the result of calorimetric measurements, as represented by the red line in Fig. 4.

This energy content increase in the radiation flux pulse is directly related to the increase in power of the radiation flux as soon as the pulse duration remains unchanged. This indicates that a further increase of the beam current density in the plasma will allow one to generate a radiation flux at a higher plasma density. For example, the use of a linear induction accelerator as a source of kiloampere REB to provide a current density level of about 10 kA/cm$^2$ will make it possible to experimentally achieve generation of radiation at a higher plasma density and correspondingly to achieve radiation frequency range of ~1 THz [31].

As seen from the spectral composition of the radiation flux presented in Fig. 3, the frequency band in the spectral region of upper-hybrid plasma oscillations is quite wide. This is explained by significant variations in plasma density in the cross-section of the plasma column and its length, where intense beam–plasma interaction occurs. In order to compare the experimentally measured radiation spectrum in this frequency band with the predictions of the theoretical model [9, 10, 13] that describes the excitation of upper-hybrid waves in a homogeneous plasma we focused on creating experimental conditions under which the density distribution is uniform both over the cross-section and along the length of the plasma column. The results of such experiments are described in the next section.

## THE RADIATION SPECTRUM AT HOMOGENEOUS PLASMA DENSITY IN A PLASMA COLUMN

In order to compare the spectral composition of the generated radiation measured in experiments with the theoretical prediction, a plasma column with a density distribution that is sufficiently uniform in its cross-section and changing slightly along its axis was created. This homogeneous plasma column was created by selecting the operating modes of pulse gas valves and a high-voltage discharge. The results of plasma density measurements obtained by optical laser diagnostics are shown in Fig. 5. This plot was obtained by averaging the measurement results over a series of nine shots with unchanged specified plasma and beam parameters. As can be seen from the graph in Fig. 5a, the linear plasma density begins to rise

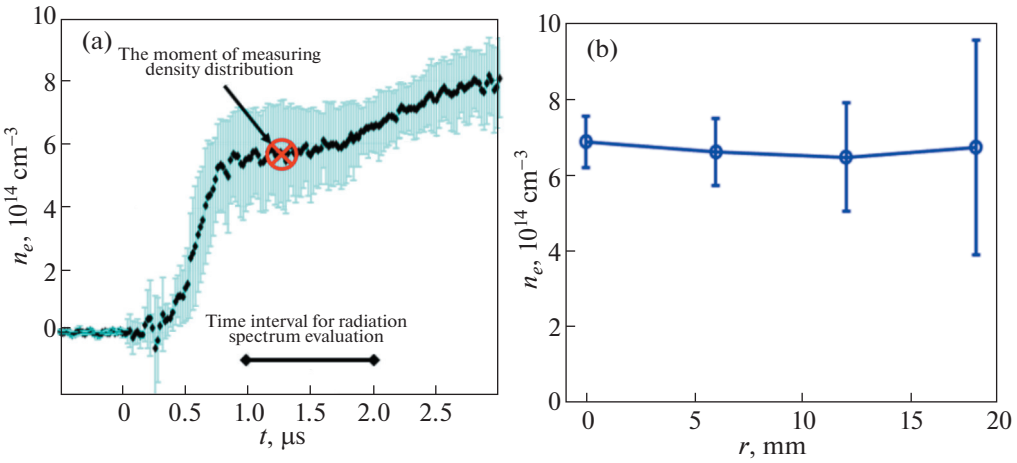


**Fig. 5.** The evolution in time of the plasma density averaged over the diameter of the plasma column, measured by Michelson interferometer at a wavelength of 10.5 μm (a); plasma density distribution along the radius of the column measured in time 1.2 μs by a Thomson scattering system at a laser wavelength of 1.053 μm (b). The time is counted from the moment of the REB injection start.

sharply from the start of the REB injection. At 0.7 μs from the start, the increase in the plasma density slows significantly, and during the time interval from 1 to 2 μs, its density becomes close to constant at the level of $(6 \pm 1) \times 10^{14}$ cm$^{-3}$. This level corresponds to the complete ionization of the initial molecular hydrogen, whose density is determined by the operating mode of the pulse valves. The density distribution along the radius of the column, as measured at 1.2 μs by the Thomson scattering system, is shown in Fig. 5b. The plasma density averaged over the plasma column cross-section for this series of shots was $(7 \pm 0.5) \times 10^{14}$ cm$^{-3}$. The close density values measured by optical diagnostics in two different cross-sections at the distance of 22 cm allow us to assert that the plasma density remained practically unchanged over such a spatial segment of the plasma column in a time interval from 1 to 2 μs from the moment of the beam injection.

Having identified the time intervals in the signals from the polychromator channels that correspond to exactly this time interval during the beam injection and by carrying out computer processing on them we constructed the emission spectrum in the generated radiation flux for a homogeneous plasma column. The result of this processing is presented in Fig. 6. As this figure demonstrates, in the frequency range from 0.1 to 0.4 THz, a high spectral radiation density is localized in the region of 0.2–0.25 THz. A two-fold lower level of spectral density was recorded in the vicinity of a frequency of 0.12 THz. In the frequency range above 0.25 THz, the spectral density is negligible compared to the two areas indicated above.

The observed spectral intervals with increased spectral density were interpreted taking the parameters of the processes measured in the facility during this series of the experiments into account. Let us compare the spectral power density measured in experiments with that calculated based on theoretical model of radiation generation with parameters that meet the experimental conditions. We associate the generation of radiation in the vicinity of 0.12 THz with the individual movement of electrons along cyclotron orbits in a magnetic field, whose induction in the plasma column ranges from 3.5 to 4.5 T, due to the corrugation structure of this field. The high spectral power density in the region of 0.2–0.25 THz is explained by the emission of the plasma at the frequencies corresponding to the branch of upper-hybrid

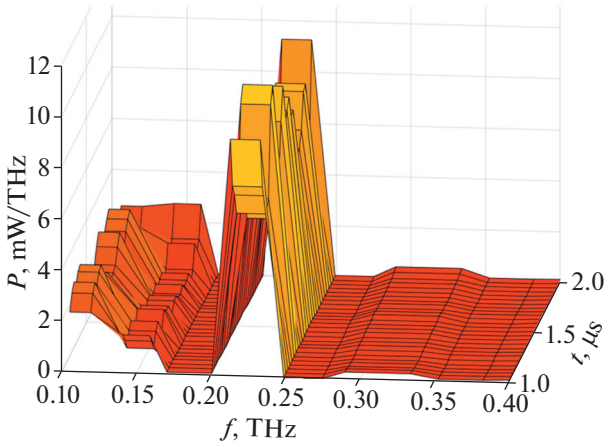


**Fig. 6.** The spectral power density in the radiation flux generated under conditions of a plasma column uniform over the cross-section (the result was obtained by averaging the recording results over a series of 9 shots under identical experimental conditions with a plasma density distribution shown in Fig. 5).

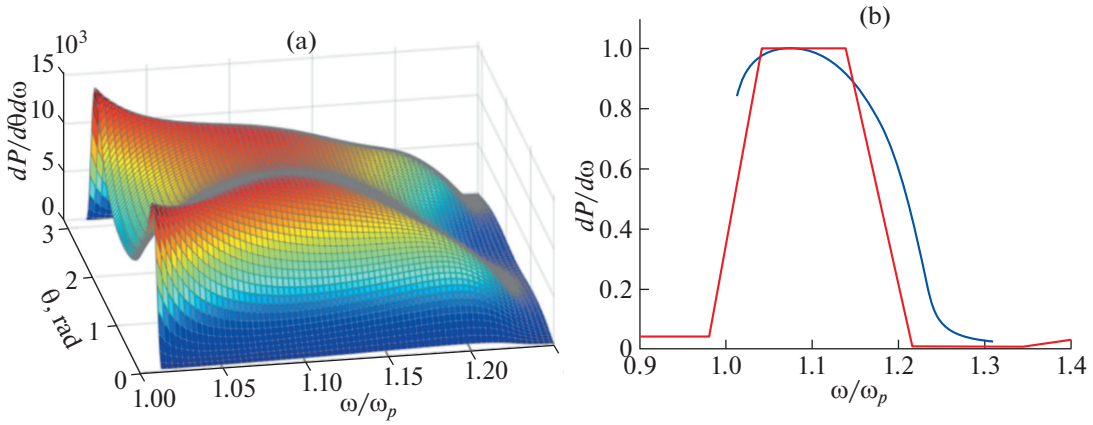


**Fig. 7.** The distribution of the spectral power density in relative units along the frequency axis in the vicinity of the Langmuir frequency ($\omega_p$). The left part of the figure, designated (a), shows the calculated angular distribution of the spectral radiation flux density in the vicinity of the frequency $\omega_p$, the position of which on the frequency axis corresponds to one. On the right half, designated (b), the blue line shows the spectral power density obtained by integrating over the angles θ of the distribution presented in (a), and the red line shows the contour of the frequency region with the maximum spectral radiation power density, constructed by the measurements results obtained with the eight-channel polychromator.

plasma oscillations. The measured value of the plasma density (6–7) × $10^{14}$ $cm^{-3}$, as well as the given value of the guiding magnetic field induction, allows us to indicate the frequency range in which upper-hybrid plasma oscillations are to be excited. This is the frequency range from the Langmuir oscillations $f_p$ = 0.22 THz to the upper cutoff frequency of this branch of plasma waves, which is $f_{uh}$ = 0.25 GHz [13].

The results of computer calculations of the spectral composition of the radiation from the plasma in the frequency range of upper-hybrid plasma oscillations performed on the base of the theoretical model described in [13] are shown in Fig. 7a, where the frequency is normalized to the plasma frequency $\omega_p$. The result of the calculations is presented here in the form of the spectral power density distribution over the angle θ, counted from the direction of the magnetic field induction.

The results of this theoretical calculation indicate that the radiation generated by the beam propagates at angles of 20–30 degrees to the direction of the guiding magnetic field. At the same time, the spectral power density integrated over angles θ is localized in the area of 1–1.2 THz frequencies normalized to $\omega_p$, which corresponds to the frequency range recorded in the experiment at 0.20–0.26 THz. Figure 7b presents the frequency range with high spectral density recorded in the experiment together with the curve demonstrating distribution of the spectral density of the radiation in the flux, calculated using the theoretical model mentioned above. A comparison of the results presented in this figure shows that the curve describing the result of calculating the spectral power density coincides well with the contour covering the region of high spectral radiation flux density, which is identified according to the experimental results.

## CONCLUSIONS

Measurements of the spectral composition and energy content in a flux of terahertz radiation generated in a magnetized plasma column with a density in the range from 4 × $10^{14}$ to 8 × $10^{14}$ $cm^{-3}$ during relaxation of a pulsed REB with a duration of a few microseconds and current density from 1 to 2 kA/$cm^2$ were carried out. It is shown that in the case of the significant inhomogeneity in the plasma density over the cross-section of the column with its average value in the vicinity of 4 × $10^{14}$ $cm^{-3}$, the spectrum of the generated radiation turns out to be quite wide. The spectral power density has a maximum in the region of 0.15–0.2 THz corresponding to the localization of the spectrum of the electron plasma waves. This flux from the plasma column end into the vacuum chamber contains the energy about 10 J at a 4 μs pulse duration. The energy content in the radiation flux from the vacuum chamber into the atmosphere through a window made of polymer material is two times lower.

A two-fold increase in the current density of the beam injected into the plasma column from 1 to 2 kA/$cm^2$ provide effective generation of a radiation flux in the plasma with a density that was also almost doubled. Experimental conditions providing the plasma density distribution uniform over column cross-section with small perturbation along its axis in a time interval ~2 μs were used. The spectral composition of the radiation measured experimentally under such conditions has a relatively narrow band of high spectral power localized in the frequency range

0.20–0.25 THz. A comparison of this experimental result with the calculated spectrum obtained in theoretical consideration of pumping the waves in the plasma with homogeneous density showed that the generation of terahertz radiation in a beam–plasma system is occurs through pumping plasma oscillations on the branch of upper-hybrid waves.

The frequency of the radiation generated in a beam–plasma system lies on the branch of upper-hybrid plasma oscillations so that an increase in the radiation frequency can be achieved by an increase of the plasma density and/or the induction of the guiding magnetic field. To achieve such an increase a linear induction accelerator that had already been created at the Budker Institute of Nuclear Physics, Siberian Branch, Russian Academy of Sciences is to be used. It provides generation of a kiloampere beam of MeV electrons, which may be compressed in the cross-section in order to achieve a current density higher than 10 kA/cm$^2$. Such a beam current density allows one to advance in a beam–plasma experiment into the region of plasma densities that are an order of magnitude greater than those described in this text, which will provide the generation of multi-megawatt radiation fluxes in the vicinity of a frequency of 1 THz.

## FUNDING

Measurements of the spectral composition of the radiation was supported by the Russian Science Foundation, project no. 19-12-00250-P. The work of I.V. Timofeev was supported by the Foundation for the Advancement of Theoretical Physics and Mathematics "BASIS."

## CONFLICT OF INTEREST

The authors of this work declare that they have no conflicts of interest.

## REFERENCES

1. A. G. Markelz and D. M. Mittleman, ACS Photonics **9**, 1117 (2022).
2. K. B. Cooper, R. J. Dengler, N. Llombart, B. Thomas, G. Chattopadhyay, and P. H. Siegel, IEEE Trans. Terahertz Sci. Technol. **1**, 169 (2011).
3. A. A. L. Michalchuk, J. Hemingway, and C. A. Morrison, J. Chem. Phys. **154**, 064105 (2021).
4. A. V. Arzhannikov, A. V. Burdakov, V. S. Koidan, and L. N. Vyacheslavov, Phys. Scr. **1982**, 303 (1982).
5. V. L. Ginzburg and V. V. Zheleznyakov, Sov. Astron. **3**, 235 (1959).
6. A. V. Arzhannikov, A. V. Burdakov, P. V. Kalinin, S. A. Kuznetsov, M. A. Makarov, K. I. Mekler, S. V. Polosatkin, V. V. Postupaev, A. F. Rovenskikh, S. L. Sinitsky, V. F. Sklyarov, V. D. Stepanov, Yu. S. Sulyaev, M. K. A. Thumm, and L. N. Vyacheslavov. Vestn. Novosib. Gos. Univ., Ser.: Fiz. **5** (4), 44 (2010).
7. A. V. Arzhannikov, A. V. Burdakov, S. A. Kuznetsov, M. A. Makarov, K. I. Mekler, V. V. Postupaev, A. F. Rovenskikh, S. L. Sinitsky, and V. F. Sklyarov, Fusion Sci. Technol. **59**, 74 (2011).
8. A. V. Arzhannikov, A. V. Burdakov, V. S. Burmasov, D. E. Gavrilenko, I. A. Ivanov, A. A. Kasatov, S. A. Kuznetsov, K. I. Mekler, S. V. Polosatkin, V. V. Postupaev, A. F. Rovenskikh, S. L. Sinitsky, V. F. Sklyarov, and L. N. Vyacheslavov, Phys. Plasmas **21**, 082106 (2014).
9. A. V. Timofeev, Phys.—Usp. **47**, 555 (2004).
10. I. V. Timofeev, V. V. Annenkov, and A. V. Arzhannikov, Phys. Plasmas **22**, 113109 (2015). https://doi.org/10.1063/1.4935890
11. V. A. Arzhannikov, I. A. Ivanov, A. A. Kasatov, S. A. Kuznetsov, M. A. Makarov, K. I. Mekler, S. V. Polosatkin, S. S. Popov, A. F. Rovenskikh, D. A. Samtsov, S. L. Sinitsky, V. D. Stepanov, V. V. Annenkov, and I. V. Timofeev, Plasma Phys. Controlled Fusion **62**, 045002 (2020).
12. A. V. Arzhannikov and I. V. Timofeev, Plasma Phys. Controlled Fusion **54**, 105004 (2012).
13. A. V. Arzhannikov and I. V. Timofeev, Vestn. Novosib. Gos. Univ., Ser.: Fiz. **11** (4), 78 (2016).
14. A. V. Arzhannikov, A. V. Burdakov, V. S. Burmasov, D. E. Gavrilenko, I. A. Ivanov, A. A. Kasatov, S. A. Kuznetsov, K. I. Mekler, S. V. Polosatkin, V. V. Postupaev, A. F. Rovenskikh, S. L. Sinitsky, V. F. Sklyarov, and L. N. Vyacheslavov, Phys. Plasmas **21**, 082106 (2014).
15. A. V. Arzhannikov, A. V. Burdakov, V. S. Burmasov, A. A. Kasatov, S. A. Kuznetsov, M. A. Makarov, K. I. Mekler, S. V. Polosatkin, S. S. Popov, V. V. Postupaev, A. F. Rovenskikh, S. L. Sinitsky, V. F. Sklyarov, V. D. Stepanov, I. V. Timofeev, et al., IEEE Trans. Terahertz Sci. Technol. **6**, 245 (2016).
16. A. V. Arzhannikov, V. S. Burmasov, I. A. Ivanov, P. V. Kalinin, S. A. Kuznetsov, M. A. Makarov, K. I. Mekler, S. V. Polosatkin, A. F. Rovenskikh, D. A. Samtsov, S. L. Sinitsky, V. D. Stepanov, and I. V. Timofeev, in *Proceedings of the 44th International Conference on Infrared, Millimeter, and Terahertz Waves, Paris, 2019.* https://doi.org/10.1109/IRMMW-THz.2019.8874408
17. D. A. Samtsov, A. V. Arzhannikov, S. L. Sinitsky, M. A. Makarov, S. A. Kuznetsov, K. N. Kuklin, S. S. Popov, E. S. Sandalov, A. F. Rovenskikh, A. A. Kasatov, V. D. Stepanov, I. A. Ivanov, I. V. Timofeev, V. V. Annenkov, and V. V. Glinskiy, IEEE Trans. Plasma Sci. **49**, 3371 (2021).
18. A. V. Arzhannikov, S. L. Sinitsky, S. S. Popov, I. V. Timofeev, D. A. Samtsov, E. S. Sandalov, P. V. Kalinin, K. N. Kuklin, M. A. Makarov, A. F. Rovenskikh, V. D. Stepanov, V. V. Annenkov, and V. V. Glinsky, IEEE Trans. Plasma Sci. **50**, 2348 (2022).
19. A. V. Arzhannikov, P. V. Kalinin, S. A. Kuznetsov, K. N. Kuklin, M. A. Makarov, S. S. Popov, A. F. Rovenskikh, D. A. Samtsov, E. S. Sandalov, S. L. Sinitsky, V. D. Stepanov, V. V. Glinsky, and I. V. Timofeev, in *Proceedings of the 46th International Conference on Infrared, Millimeter and Terahertz Waves, Chengdu, 2021.* https://doi.org/10.1109/IRMMW-THz50926.2021.9567120
20. A. V. Arzhannikov, I. A. Ivanov, P. V. Kalinin, and A. A. Kasatov, J. Phys.: Conf. Ser. **1647**, 012011 (2020).

21. A. V. Arzhannikov, V. B. Bobylev, V. S. Nikolaev, S. L. Sinitsky, M. V. Yushkov, and R. P. Zotkin, in *Proceedings of the 1992 9th International Conference on High-Power Particle Beams, Washington, DC, 1992*, Vol. 2, p. 1117.

22. A. V. Arzhannikov, M. A. Makarov, D. A. Samtsov, S. L. Sinitsky, and V. D. Stepanov, Nucl. Instrum. Methods Phys. Res., Sect. A **942**, 162349 (2019).

23. V. S. Burmasov, V. B. Bobylev, A. A. Ivanov, S. V. Ivanenko, A. A. Kasatov, D. A. Kasatov, E. P. Kruglyakov, K. N. Kuklin, S. S. Popov, V. V. Postupaev, E. A. Puryga, A. F. Rovenskikh, and V. F. Sklyarov, Instrum. Exp. Tech. **55**, 259 (2012).

24. S. S. Popov, L. N. Vyacheslavov, M. V. Ivantsivskiy, A. V. Burdakov, A. A. Kasatov, S. V. Polosatkin, and V. V. Postupaev, Fusion Sci. Technol. **59**, 292 (2011).

25. A. V. Arzhannikov, M. A. Makarov, P. A. Kalinin, A. A. Kasatov, K. N. Kuklin, S. S. Popov, D. A. Samtsov, E. S. Sandalov, and S. L. Sinitskii, in *XLVIII International Zvenigorod Conference on Plasma Physics and Controlled Fusion, Zvenigorod, 2021*, Book of Abstracts, p. 182.

26. V. E. Rogalin, I. A. Kaplunov, and G. I. Kropotov, Opt. Spectrosc. **125**, 1053 (2018).

27. A. V. Arzhannikov, I. A. Ivanov, S. A. Kuznetsov, D. A. Samtsov, P. A. Lazorskiy, and A. V. Gelfand, in *Proceedings of the 2021 IEEE 22nd International Conference of Young Professionals in Electron Devices and Materials, Souzga, 2021*, p. 101.

28. N. I. Zaitsev, E. V. Ilyakov, Yu. K. Kovneristyi, G. S. Korablev, I. S. Kulagin, I. Yu. Lazareva, V. I. Tsalolikhin, and V. V. Shulgin, Instrum. Exp. Tech. **35**, 283 (1992).

29. A. V. Arzhannikov, S. L. Sinitskii, D. A. Samtsov, E. S. Sandalov, S. S. Popov, M. G. Atlukhanov, M. A. Makarov, P. V. Kalinin, K. N. Kuklin, A. F. Rovenskikh, and V. D. Stepanov, Plasma Phys. Rep. **48**, 1080 (2022).

30. A. V. Arzhannikov, A. V. Burdakov, V. S. Burmasov, V. S. Koidan, V. V. Konyukhov, K. I. Mekler, A. I. Rogozin, and L. N. Vyacheslavov, in *Proceedings of the 3rd International Topical Conference on High Power Electron and Ion Beam Research and Technology, Novosibirsk, 1979*, p. 29.

31. A. V. Arzhannikov, S. L. Sinitskii, D. A. Starostenko, P. V. Logachev, P. A. Bak, D. A. Nikiforov, S. S. Popov, P. V. Kalinin, D. A. Samtsov, E. S. Sandalov, M. G. Atlukhanov, A. N. Grigor'ev, S. O. Vorob'ev, D. V. Petrov, and R. V. Protas, Sib. Fiz. Zh. **18** (1), 28 (2023).